Inclusive Jet Production and Virtual Photon Structure.

Tania R. Ebert
(for the H1 Collaboration)

Oliver Lodge Laboratory, University of Liverpool, P.O. Box 147, Liverpool, L69 3BX, U.K.

Abstract. The transition between photoproduction and deep-inelastic scattering is investigated in jet production, using data collected by the H1 experiment. Measurements of the inclusive jet cross sections $\mathrm{d}\sigma_{\gamma^* p}/\mathrm{d}E_t^*$ and $\mathrm{d}\sigma_{\gamma^* p}/\mathrm{d}\eta^*$ in the $\gamma^* p$ frame are presented for $0 < Q^2 < 49\,\mathrm{GeV}^2$ and $0.3 < y < 0.6$. The interpretation of the results in terms of the structure of the virtual photon is discussed. A measurement of the energy flow in the direction of the photon as a function of Q^2 is shown.

INTRODUCTION

In the photoproduction of jets [1], the cross-section is dominated by "resolved" processes, in which the photon fluctuates into a system of partons, one which subsequently interacts with a parton from the proton leaving the remainder to form the photon remnant. "Direct" interactions occur when the photon couples directly to a parton in the proton.

In contrast, it is usual to consider that the only contribution to jet production in deep inelastic scattering (DIS) is from direct interactions, with the proton probed by a structureless photon with virtuality Q^2. However, if high transverse momentum (p_t) jets are produced with $p_t^2 \gg Q^2$, it is possible to interpret the data in terms of the partonic structure of the virtual photon [2]. Parton densities in the virtual photon are expected to be suppressed [3,4] with increasing Q^2 until direct processes dominate at $Q^2 \sim p_t^2$.

EVENT SELECTION

A detailed description of the H1 detector can be found elsewhere [5]. The analysis [6] is based on data taken in 1994 and 1995. Photoproduction data with $Q^2 < 10^{-2}\,\mathrm{GeV}^2$ and DIS data with $0.65 < Q^2 < 49\,\mathrm{GeV}^2$ were used. To enable comparisons between the datasets, the kinematic range was restricted to $0.3 < y < 0.6$.

The event kinematics were reconstructed from the scattered electron 4–vector. Jets were reconstructed in the $\gamma^* p$ frame using a k_T clustering algorithm [7] with a hard scale of 3 GeV. Particles were either associated to jets or to the photon or proton remnant. The jets were required to have a transverse energy $E_t^* > 4(5)$ GeV for the DIS (photoproduction) data and a pseudorapidity -2.5 $< \eta^* <$ -0.5.

QCD MODELS

The data is compared to the QCD event generator HERWIG [8]. The direct photon contribution to this model is the sum of the boson–gluon fusion and QCD Compton processes. The evolution of the photon structure with Q^2 is modelled using the Drees–Godbole parameterization [4] where the quark densities in a photon of virtuality Q^2 probed at a scale p_t^2 are related to those of a real photon by:

$$\begin{aligned} f_{q/\gamma^*}(x, p_t^2, Q^2) &= f_{q/\gamma}(x, p_t^2, 0) L(p_t^2, Q^2, \omega) \\ &= f_{q/\gamma}(x, p_t^2, 0) \frac{\ln\{(p_t^2+\omega^2)/(Q^2+\omega^2)\}}{\ln\{(p_t^2+\omega^2)/\omega^2\}} \end{aligned}$$

An analogous relation exists for the gluon density, with L replaced by L^2. ω is the value of Q^2 above which the suppression of the parton densities becomes significant. We use a value of $\omega = 1\,\mathrm{GeV}^2$ and refer to this throughout as the HERWIG DG model.

For events at $Q^2 = 0\,\mathrm{GeV}^2$ we include a "soft–underlying event", to model remnant–remnant interactions, in 15% of resolved events. This gives a good description of the jet profiles observed in the data.

For the proton parton density, the GRV94 HO (DIS) [9] parameterization, which gives a good description of the measured F_2 for $Q^2 > 1\,\mathrm{GeV}^2$ [10], was used. The GRV-G HO (DIS) [11] parton density was used for the real photon.

The DIS generator LEPTO [12] was also used for comparison with the data.

RESULTS

Inclusive Jet Cross-Section

The jet cross-sections are corrected for detector effects and full systematic errors have been evaluated.

We define the $\gamma^* p$ jet cross–section as:

$$\sigma_{\gamma^* p \to jet+X} = \frac{\sigma_{ep \to e+jet+X}}{F_{\gamma/e}} \qquad (1)$$

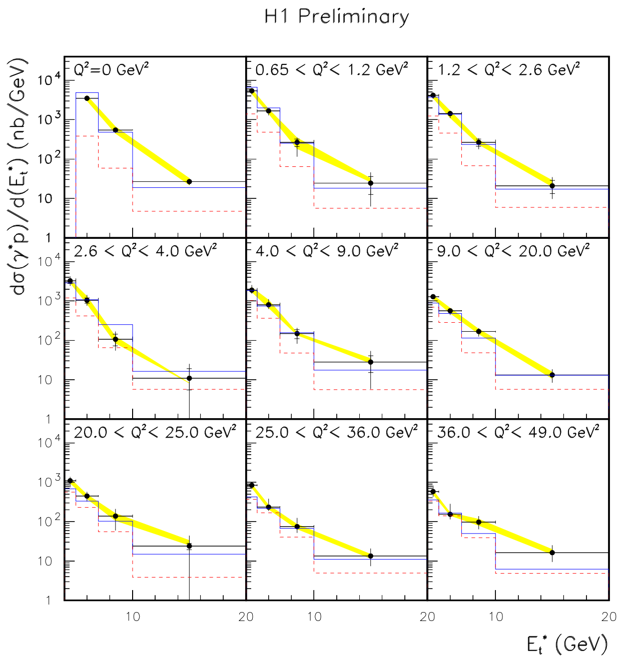

FIGURE 1. $\mathrm{d}\sigma_{\gamma^* p}/\mathrm{d}E_t^*$ for jets with $-2.5 < \eta^* < -0.5$. The data points, with the inner error bars indicating the statistical error, the outer error bar the statistical and systematic errors added in quadrature and the shaded band representing the normalization error, are compared to the HERWIG DG model (solid line) and the direct contribution to this model (dashed line).

where the flux of virtual photons ($F_{\gamma/e}$) is given by the Weizsäcker–Williams approximation [13] integrated over y and Q^2.

Figure 1 shows the inclusive $\gamma^* p$ jet cross–section $\mathrm{d}\sigma_{\gamma^* p}/\mathrm{d}E_t^*$. The direct photon contribution from HERWIG significantly underestimates the data at low Q^2 The HERWIG DG model which includes a resolved component of the virtual photon is able to describe the data.

The jet cross-section $\mathrm{d}\sigma_{\gamma^* p}/\mathrm{d}\eta^*$ for jets with $E_t^* > 5\,\mathrm{GeV}$ is shown in figure 2. The data are compared to the HERWIG DG model and the direct photon contribution to this model. Again, the direct photon processes from HERWIG underestimate the jet cross–section at low Q^2, but the data is described by the HERWIG DG model.

Figure 3 shows the Q^2 dependence of the inclusive $\gamma^* p$ jet cross-section at fixed jet E_t^*. For $E_t^* < 10\,\mathrm{GeV}$ there is a significant decrease of the jet cross-section with increasing Q^2. As expected from the first order matrix elements, the $\gamma^* p$ cross-section for the direct processes from HERWIG is independent of Q^2 when $Q^2 < P_t^2$, in contrast to the behaviour seen in the data. The data are described by the HERWIG DG model.

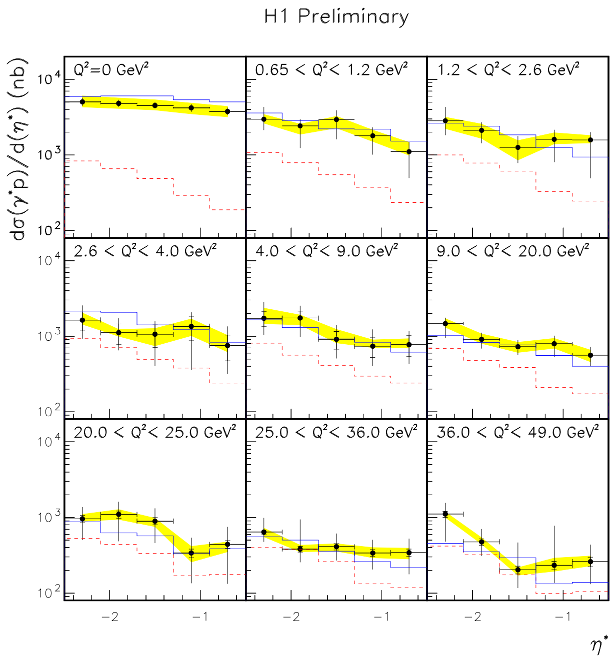

FIGURE 2. $d\sigma_{\gamma^* p}/d\eta^*$ for jets with $E_t^* > 5\,\mathrm{GeV}$. The data points, with the inner error bars indicating the statistical error, the outer error bar the statistical and systematic errors added in quadrature and the shaded band representing the normalization error, are compared to the HERWIG DG model (solid line) and the direct contribution to this model (dashed line).

The Photon Remnant.

The jet algorithm assigns particles to a photon remnant. We define f as the fraction of the incident photon's energy which is reconstructed in the photon remnant jet.

Figure 4 shows the uncorrected distribution of f in the data, as a function of Q^2, for events with at least one jet with $E_t^* > 5\,\mathrm{GeV}$ and -2.5 $< \eta^* <$ -0.5. At $Q^2 = 0\,\mathrm{GeV}^2$, where resolved photon processes dominate the cross-section, most of the events contain a photon remnant with a significant fraction of the incident photon's energy. Conversely, at the highest Q^2 values, where direct processes dominate, f is peaked at zero. The distribution from LEPTO (after detector simulation) is peaked at zero for all Q^2, as expected for a model which includes only direct photon processes. At low Q^2, the data agrees with the HERWIG DG model, and at high Q^2 with LEPTO. The change in the distribution of f with Q^2 is consistent with the picture of a resolved photon contribution which is suppressed with Q^2.

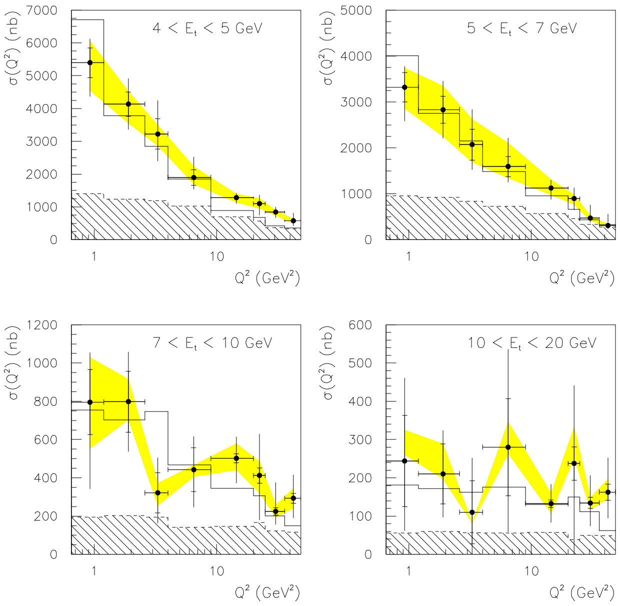

FIGURE 3. The inclusive jet cross-section $\sigma(Q^2)$ for jets with -2.5< η^* <-0.5. The data points, with the inner error bars indicating the statistical error, the outer error bar the statistical and systematic errors added in quadrature and the the shaded band representing the normalization error, are compared to the HERWIG DG model (solid line) and the direct contribution to this model (hatched histogram).

CONCLUSIONS

The inclusive jet cross-sections $\mathrm{d}\sigma_{\gamma^* p}/\mathrm{d}E_t^*$ and $\mathrm{d}\sigma_{\gamma^* p}/\mathrm{d}\eta^*$ have been measured in the kinematic range $0.3 < y < 0.6$ and $0 < Q^2 < 49\,\mathrm{GeV}^2$.

Models in which the photon is treated as a pointlike object fail to describe the data when $P_t^2 \gg Q^2$ and the virtual photon can be resolved. A model which includes a resolved component of the photon suppressed with Q^2 according to the Drees–Godbole parameterization describes the data.

It has been established that the energy assigned to the photon remnant is large at low Q^2 and decreases with increasing Q^2, consistent with the picture of a resolved photon component which is suppressed with its increasing virtuality.

REFERENCES

1. H1 Collab., S. Aid et al., Z. Phys.**C70** (1996) 17.
2. T. Uematsu and T. Walsh, Phys. Lett. **101B** (1981) 263.
   T. Uematsu and T. Walsh, Nucl. Phys. **B199** (1982) 93.
3. F. Borzumati and G. Schuler, Z. Phys. **C58** (1993) 139.
4. M. Drees and R. Godbole, Phys. Rev. **D50** (1994) 3124.

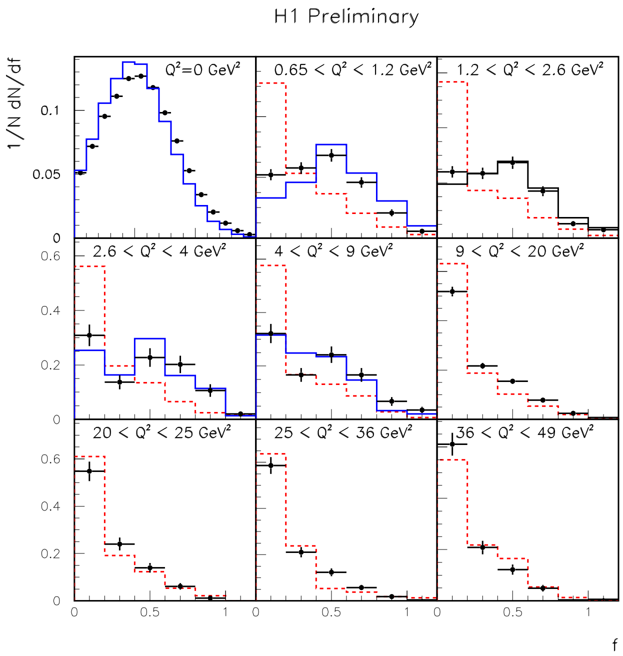

FIGURE 4. The fraction of the incident photon's energy which is reconstructed in the photon remnant jet for events with at least one jet with $E_t^* > 5\,\mathrm{GeV}$ and -2.5 $< \eta^* <$ -0.5. The uncorrected data is compared to the HERWIG DG model (solid line) and to LEPTO (dashed line) after detector simulation.

5. H1 Collaboration, I. Abt et al., Nucl. Instr. and Meth. **A386** (1997) 310 and **A386** (1997) 348.
6. H1 Collaboration, "Low Q^2 Jet Production at HERA and Virtual Photon Structure", to be published
7. S. Catani, Yu.L. Dokshitzer and B.R. Webber Phys. Lett. **B285** (1992) 291.
8. G. Marchesini, B.R. Webber et al., Comp. Phys. Comm. **67** 1992 465
9. M. Gluck, E. Reya, A. Vogt, Z. Phys. **C67** (1995) 433
10. H1 Collaboration, DESY-97-042, submitted to Nucl. Phys. **B**
11. M. Gluck, E. Reya, A. Vogt, Phys. Rev. **D45** (1992) 3986
12. G. Ingelman, Proc. of the Workshop on Physics at HERA, 1991, Vol. 3, 1366.
13. C.F. v. Weizsäcker, Z. Phys. **88** (1934) 612
    E.J. Williams, Phys. Rev. **45** (1934) 729.